Opt Quant Electron (2017) 49:140
DOI 10.1007/s11082-017-0957-z

Cytotoxicity and apoptotic effects of polymer coated copper oxide nanoparticles synthesized via SLM in mesenchymal stem cells

Igor Volyanski[1] · Stanislaw Volchkov[2] · Igor Shishkovsky[1,2,3]

Received: 3 August 2016 / Accepted: 21 February 2017 / Published online: 14 March 2017

Abstract Copper oxide inclusions were incorporated in polymer matrix (polycarbonate/PC/, polyetheretherketone/PEEK/etc.) during selective laser melting process. The aim of this study was to observe the cytotoxicity and apoptotic effects of the copper oxide nanoparticles on a culture of multipotent mesenchymal stem cells after 3D laser bioprinting. The matrices of polymer coated Cu/CuO nanoparticles (<100 nm) were investigated by X-ray diffraction analysis and scanning electron microscopy techniques. The viable cells were counted using light microscopy. It was determined that Cu/CuO nanoparticles have a strong toxic effect on PC matrix unlike background high biocompatible PEEK matrix, which smoothes apoptotic effect. We also discuss the implications of our findings regarding the effects of the intrinsic toxic properties of Cu/CuO nanoparticles, and concluded that the apparent toxicities of metal oxide NPs can largely be understood as a matter of particle toxicity.

Keywords 3D laser bioprinting · Copper nano particles (NP) · Biopolymers · Multipotent mesenchymal stem cells (MMSC) · Cytotoxicity

This article is part of the Topical Collection on Fundamentals of Laser Assisted Micro- and Nanotechnologies.

Guest edited by Eugene Avrutin, Vadim Veiko, Tigran Vartanyan and Andrey Belikov.

✉ Igor Volyanski
i.volyansky@gmail.com

✉ Igor Shishkovsky
shiv@fian.smr.ru

[1] Ecole Nationale d'Ingénieurs de Saint-Etienne (ENISE), 58 rue Jean Parot, 42023 Saint-Étienne Cedex 2, France

[2] Samara State Medical University, Chapaevskaya Str. 89, Samara, Russia 443099

[3] P. N. Lebedev Physical Institute of Russian Academy of Sciences (RAS), Samara Branch, Novo-Sadovaja Str. 221, Samara, Russia 443011

1 Introduction

Nanoparticles (NPs) in their pure form are rarely used for therapeutic purposes. Usually they are encapsulated and/or placed in biologically inert matrixes (oligomers or polymers, including those of natural origin) with the view of controlling possible toxic influence, raising its physicochemical stability and creating immobilization conditions on the surface of drugs delivery system (DDS) capsules or matrixes. The problem of the DDS manufacturing could be successfully solved by the 3D bioprinting methods (Shishkovskii et al. 2012). Promising biomedical platform technologies are microcapsulation, technology for manufacturing of matrix, multilayered and coated tablets and capsules. The targeted DDS is one more promising sphere for medical application of NPs. The nano size may result in several times' increase of drug activity and also in reinforcement of therapeutic characteristics. Its main advantages are ordering of the drug toxic effect on other organs and systems, possibility to direct and retain the drug-containing NPs in a certain place with the help of electromagnetic fields.

Applications of Cu/CuO NPs are very important in antibacterial coatings, in catalyst or solar batteries (Chang et al. 2012; Shafagh et al. 2015). The Cu/CuO NPs induce generation of reactive oxygen species (ROS) oxidative stress which causes DNA damage and increases death receptor expression (Yang et al. 2009). Apoptosis is a key mechanism in cancer development and progression. Cancer cells avoid apoptosis and continue to propagate. So the apoptosis is mediated by ROS generation and oxidative stress (Ott et al. 2007; Shafagh et al. 2015).

The laser 3D bioprinting has a great indisputable potential for fabricating the DDS (Shishkovsky 2012) with a predefined and reproducible external and internal surface morphology that could be used in medical applications. The advantage of the Selective Laser Sintering (SLS) technique as one related to this technology, consists in the opportunities it provides to fabricate the objects additively, on a layer-by-layer basis, directly from a 3D computer-designed model of the real functional implant, with no need in specialized moulds, dies or other tooling (Leong et al. 2001; Kanczler et al. 2009; Ogura et al. 2004; Shishkovskii et al. 2011, 2012; Zinger et al. 2004; Engel and Bourell 2000; Das et al. 1999; Williams et al. 2005).

The implant testing on cellular cultures is widespread as the first stage of biological testing for biocompatibility and toxicity of implants (Murray et al. 2007). Pluripotent mesenchymal stromal stem cells (MSSC) are the most promising autologous material for the cell therapy and tissue engineering, since they can be found practically inside any conjunctive tissue (Volchkov et al. 2009; Salamon and Toldy 2009). The MSSC usage allows on the cell level to show the implant of targeting material properties, for instance its influence on the connective tissue cells. Provided that the toxic effects are possible to manage, it is possible to estimate the adhesion properties, velocity and depth of the stem cells ingrowth in the implant, and hence—to prognosticate the degree of integrity of the DDS with the living tissue (Nirmalanandhan and Sittampalam 2009). The present study purpose was to evaluate using cell viability, oxidative stress and apoptosis detection, proliferative activity and phenotypic changes during the testing.

2 Materials and experimental procedure

2.1 Materials preparation

The objects of the study were heat-treated polycarbonate (PC graded LET, Dzerginsk, Russian Federation) and polyetheretherketone (PEEK, Victrex Co., UK). The polymeric fraction particles were selected to have a size of 50 μm, comparable with the laser spot diameter. That guaranteed a high packaging density of the particles in the initial nanopolymer composition and hence—a good quality of its sintering. The copper nanoparticles (NPs) were prepared at the Institute of Structural Macrokinetics and Material Sciences (ISMMS) of RAS by means of the levitation jet technique. The mean size values of Cu particles were 76–100 nm. The Cu percentage and specific surface area of the powders were measured 96.8/3.4 w.% Cu (bal., CuO)/m^2/g, respectively. The Cu/CuO NPs were used as fillers for the polymeric matrix. Polymeric nanocomposites were prepared for the sintering in the following ratios by weight (the first proportion is for the NPs): 1:10, 1:20, 1:50.

2.2 SLS equipment

A continuously operated YAG:Nd^{+3} laser (1.06 μm wavelength) was used to carry out the SLS process. The beam power P ranged from 4 to 10 W. The laser beam was scanning the powder surface by meander; the width between laser passages was equal 70 μm as the laser beam diameter. That guaranteed a high packaging density of the particles in the polymer nanocomposition and hence - a good quality of its sintering under laser influence (LI). The optic facility was used with the beam focal length of 147 mm and shift of 25 mm from the bottleneck (Shishkovsky 2009). Layerwise laser sintering process was performed in a specially designed camera in Ar or in the air. As a result of the laser sintering (the equipment and optimal regimes of the layerwise SLS method are described in (Shishkovskii et al. 2012) for biological experiments both plain porous samples of matrices sized $\sim 10 \times 10 \times$ d mm, where d—is a monolayer thickness ($\sim$0.5–1 mm depending on the sintering regime, Fig. 1a, b) and three dimensional (3D) samples were obtained (Fig. 1c). According to the earlier developed technique (Shishkovskii et al. 2011), we modeled the

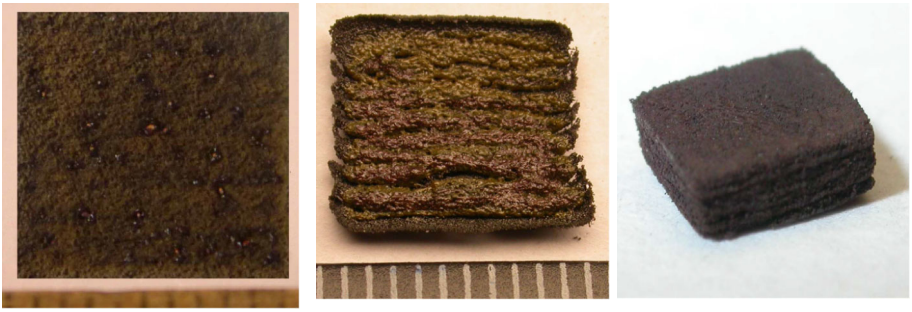

Fig. 1 The SLS of the monolayers (**a**, **b**) and 3D sample (**c**) with nano inclusions of copper. LI regimes and mixtures are shown. All the 2D and 3D samples have area of surface $\sim 10 \times 10$ mm. **a** Cu + PC = 1:10; $P = 8.6$ W, v = 10 cm/s. **b** Cu + PEEK = 1:20; $P = 4.5$ W, v = 14 cm/s. **c** Cu + PC = 1:10, $P = 8.7$ W, $v = 16$ cm/s

external appearance of the porous matrices by using the CAD-CAE prior to the laser synthesis process. Previously experiments showed (Shishkovsky and Scherbakov 2012) that SLS regimes mixture ratio (Fig. 1a, c) are more optimal for monolayer and 3D sample preparation due to better sinterability of the layers to each others. They were used in the following medical tests.

The sample shown in Fig. 1b seems inacceptable to us, for its surface is significantly rough, and the roughness is comparable with the size of certain passages of LI. This makes problems for applying the following layers in the layer by layer SLS.

2.3 Characterization of the Cu/CuO NPs

After the etching, cross sections of the multi-layered sintered samples were subjected to microstructural analysis with the optical microscope (Neophot 30 M, Carl Zeiss) equipped with a digital camera. The phase composition of the synthesized structures was determined with the x-ray diffraction (XRD) using a DRON-3 diffractometer in the Co-K_α radiation. The morphology of the laser sintered layers after the SLS was studied with a LEO 1450 scanning electron microscope (Carl Zeiss Company) equipped with an energy-dispersive x-ray analyzer (INCA Energy 300, Oxford Instruments).

2.4 Cell culture

For medical testing we used a pure growth medium for the reference group. A pure growth medium with stem cells and without the samples was used as a control group (reference group). All the samples obtained by the SLS process from polymer + nanoparticles of copper oxide and inserted into the growth medium with stem cells were considered as testing groups. All 3D printed samples were preliminarily washed clean in a sterile phosphate salt buffer (PBS) by means of reiterated immersion and active stirring of the materials in the solution. The washed materials were sterilized in a Sterident steam sterilizer at the temperature of 121 °C and pressure of 120 кPa for 20 min. The MMSC of the third passage were chosen. The cells were obtained from an adult donor's bone marrow, after the subscription of an informed consent to donate biological material according to the international laws. The cell isolation was accomplished on the Ficcol consistence gradient 1.033. The inoculation was fulfilled in all the groups under consideration in concentration of 37.5×10^4 cells per 1 cm^2 of the culture plastic. For the temperature and atmosphere equilibration, the sterile investigated materials were injected into the culture medium, 20 min. before the inoculation of testing groups.

The cultivation lasted for 17 days with the use of standard nutrient mediums such as aMEM (Sigma), 2 mM alanil-glutamine (Invitrogen Co.) and 10% selected calf serum (Gibco Co.) by scheme shown in Fig. 2. The nutrient medium was changed every 4 days or at the moment when the medium pH indication altered. We used 44 samples for medical tests. The term "series" (there were four) means number of samples fabricated under similar regime of the LI.

A daily morphology and morphometry were carried out for every group and every series of the experiment. The cells area was estimated with the AxioObserverA1 hardware and software package produced by CarlZeiss by using AxioVision software. The cluster analysis of the culture was accomplished on the ImageJ and ImageProPlus bundled software, and the cells were divided into groups according to their pixel density per object. The immunophenotyping was conducted on a running FACSCanto (BectonDickinson Co.) cytofluorometer directly before the inoculation and after the cells removal on the 0th and

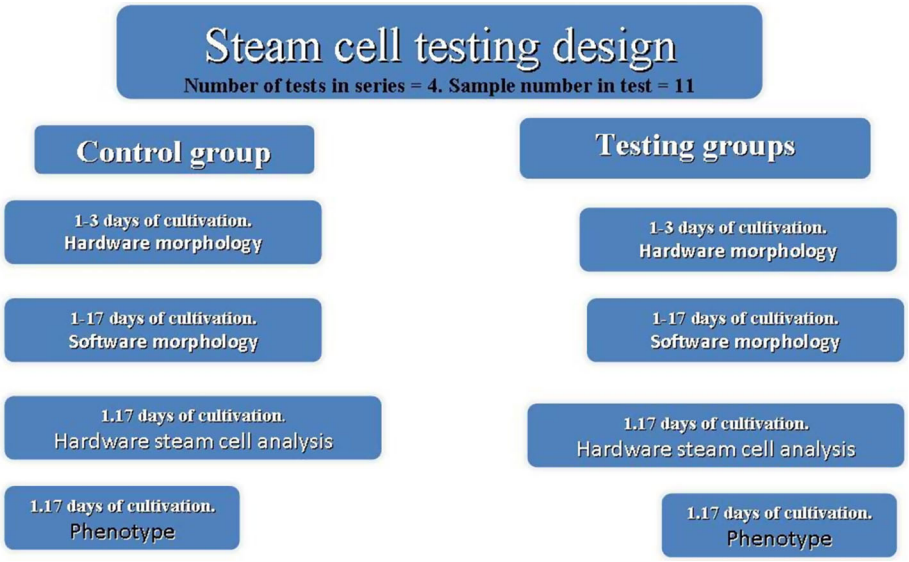

Fig. 2 Scheme of MSSC culture

17th day of cultivation. The following antigens were studied: CD 44, CD 73, CD 90, CD 105, CD 14, CD 34, CD 45, HLA-DR.

The cells calculation and proliferate activity count were performed for the 1st, 3rd and 4th series of all the groups of experiments by using a bundled Vi-Cell XR software made by Becman Coulter, before the inoculation and at the end of cultivation. The proliferative activity was estimated according to the formula: $X = [\log10(NH) - \log10(NI)]/\log10(2)$, where NH is the quantity of cells at the time of an inoculation, NH1 – the accretion of the cells quantity. On the basis of this formula, the data on the culture duplications number during the cultivation were obtained. It is convenient to estimate the speed of reduplication (i.e. duplications per hour) during the calculated quantity of duplications, using the following formula: $X = Ct/Dt$, where Ct is duration of cultivation (an hour), Dt – number of the culture duplications. The statistical data processing was accomplished using the Student's t-criterion, and all the values of $p < 0.05$ were considered significant.

3 Results and discussion

3.1 Physicochemical characteristics of the Cu/CuO NPs

Our previous studies had been shown that polymer blends with copper nano inclusions demanded less energy input under the laser sintering than those with micro inclusions. It was determined that monolayers from PC with nano copper are more durable then with micro size copper. The optimal regimes of laser sintering in PC + Cu mixtures for one monolayer were found also and later it was used for the 3D sample fabrication.

Figure 1 presents results of layer-by-layer manufacturing of 3D porous parts from PC-Cu and PEEK-Cu powder compositions. As it is visible, nano size additives of copper in PC (Fig. 1a) provide more solid samples, than copper in PEEK (Fig. 1b) under similar

laser energy input in the powder mixture. Nevertheless, in both cases on the surface of the 2D and 3D samples we observed an undesirable copper coagulation, which was intensified with the laser energy increasing.

Figure 3a, b shows the surface structure of materials obtained after the liquid-phase laser sintering of PEEK-Cu mixtures. In Fig. 3a four passages of the LI are clearly visible on the surface of the powder mixture. On the sides of the photo some reach-through pores are visible, they are black in color, have size of about 200-300 μm and length of about 1–2 mm. Light-red inclusions going angularly from bottom to the top of the photo are copper particles. Their heterogeneous distribution over the matrix is visually clear. White sites with greenish background are the polymer matrix. At a greater magnification (Fig. 3b) single passage of the LI is shown, it has a width of about 400 μm. It also has black points on the surface, which are micro pores sized 30–50 μm. Microstructure of copper (Fig. 3b) is well-marked present on the common light background of polymer.

Figure 4a–d shows the X-ray diffraction patterns obtained for PC + Cu compositions. The first curve on the Fig. 4a) shows the powder content without a laser treatment. For nanosized copper—PC (Fig. 3b–d), the patterns were consistent with those of standard Cu and CuO cubic and monoclinic phases, respectively. Moreover, the XRD patterns for PC + nano Cu reported about CuO_2 oxide also (diffraction peaks (220, 311?)), which is nearly absent in initial Cu/CuO blend from the ISMMS. Actually, near the main peak (111) of copper, an unresolved peak in nano compositions is determined, which persist on the diffractograms after the laser treatment (marked as "±"). In our opinion, this may be an amorphous part of nano copper powder. Regime for image in Fig. 1c and for curve in Fig. 4c was similar. Comparison of peak intensity distribution (Fig. 4b–d) allows to maintain that smart variation of SLS regimes is not significant influent on the phase structure of sintered samples.

Figure 5 shows the inner structure of the 3D parts obtained by liquid-phase laser sintering of PC-Cu mixtures. Sub nano structure of copper (Fig. 5) is well-marked on the common black background of polymer. The estimations gave the average grain size from 200 up to 500 nm (Fig. 5) that is slightly higher as compared to the initial value (90–100 nm).

The SEM results with EDX analysis suggest that the growth mechanism for the metal core–polymer shell structures is also applicable in our case. The formation of the PC shell structure is clearly seen in Fig. 5. It seems reasonable to assume that the polymer molecules dissolve in the Cu particles and, and if once the particle becomes supersaturated with

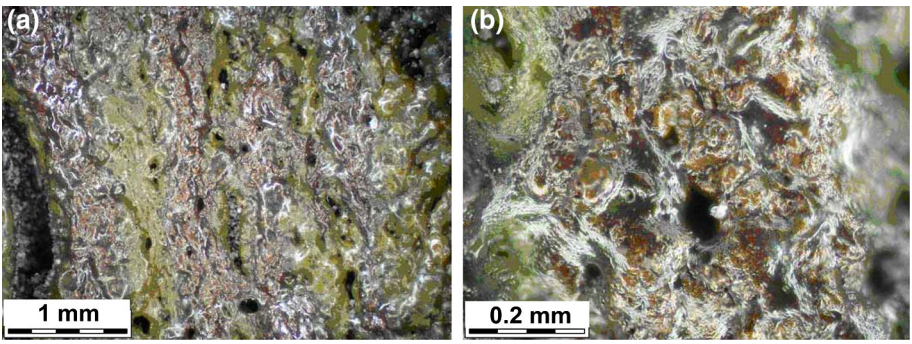

Fig. 3 OM micrographs showing the typical microstructures after the SLS on nano Cu/CuO + PEEK monolayer surface: **a** magnification ×25; **b** magnification ×250

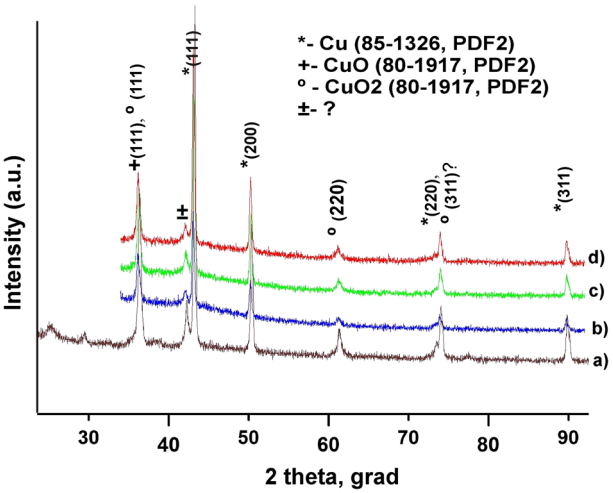

Fig. 4 XRD patterns in PC + nano Cu/CuO system = 10:1: *a* without LI; *b–d* after SLS process: *b* $P = 11$ W, v = 28 cm/s; *c* $P = 8.7$ W, v = 16 cm/s,*d* $P = 6.2$ W, v = 8 cm/s, respectively

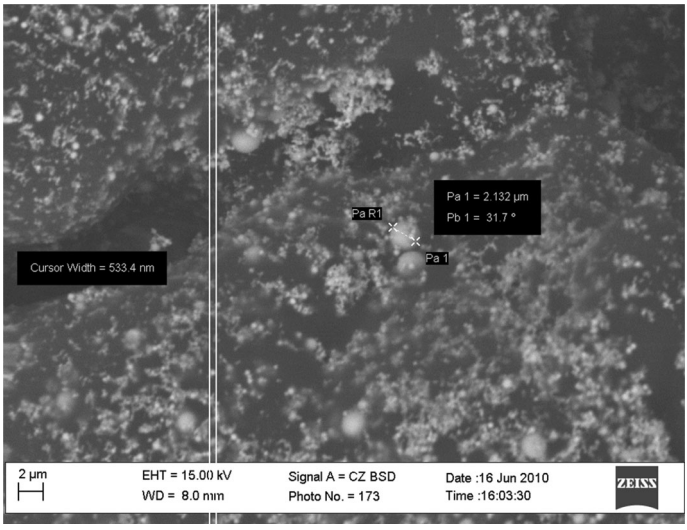

Fig. 5 SEM images of the laser sintered surface for Cu + PC mixtures with nano size copper. Content and LI regimes are shown on the Fig. 1a

carbon, then the nano size particles start to precipitate on the metal surface thus forming graphitic layers, that normally occurs at lower temperatures.

3.2 Cytotoxicity behavior of the Cu/CuO NPs

The immunophenotype of the cells was shown on the stromal markers where CD73, CD 44, CD 90, CD 105 turned out to be positive, and haemopoietic markers where CD14, CD 34, CD 45, HLA-DR, 106 turned out to be negative. The MMSC differentiation potential

was determined by means of: (1) adipogenic differentiation, where it was proved by a positive coloration response to red oil; (2) osteogenic differentiation, where it was proved by a positive coloration response to alkaline phosphatase; (3) chondrogenic differentiation, here it was proved by a positive coloration response to aggrecan.

Figure 6c–h shows a typical data of the MMSC morphological analysis near the 2D scaffolds during the testing study. The black impregnations in the photos are the breakaway fragments of the scaffolds. As it's evident from the comparison with control results (Fig. 6a, b), the situation in Fig. 6c–h was very dramatically during the period of testing. The culture density near the matrix decreased day by day.

On the second day visual inspecting (Fig. 6c) of the culture shown evident change of the matrix color from orange to black shot with violet, which is a sign of pH change to alkaline. By microscopy a lot of dead (round) cells near the studied material was observed, while the living cells were vanishingly few. Hereinafter (Fig. 6d–h) the matrix turned to be strongly alkaline with a lot of microscopically revealed dead cells and no of living ones near the studied material. So the PC-Cu/CuO system demonstrated a direct toxic effect due to making the matrix alkaline and consequent death of the cells.

In the next 10 days test (Fig. 7) using different tinctures (CFSE—Carboxyfluoresceinsuccinimidyl ester и DAPI—4′,6-Diamidino-2-phenylindole) we compared the viability of MSSC in PC-Cu/CuO and PEEK-Cu/CuO systems. It is known that CFSE—staining agent for cytoplasm, a DAPI—is stem cell staining agent. For PC is know as a bioinert poliymer, we used PEEK which is biocompatible for binding matrix. In the PC-Cu/CuO system (Fig. 7a) dead cells (apoptosis) were observed on the plastic. There were also many small dispersed particles, which can be sequence of bacterial contamination. Meanwhile in the PEEK-Cu/CuO (Fig. 7b–d) system the fluorescent photo shown round compartments of the cells and also nuclei (DAPI -Fig. 7d) in the same field as the colored by CFSE. Possible there was an agglomeration of cells on the material. So we can assume that the PEEK biocompatible matrix "protects" the MSSC from the toxic effects of the Cu-particles. We plan to repeat the study to reassure the quantitative rates of the cell death. However it is evident that alternation of PEEK and PC matrices can be a way of regulating the cells' death, which is useful for medical applications (targeting and drug delivery systems).

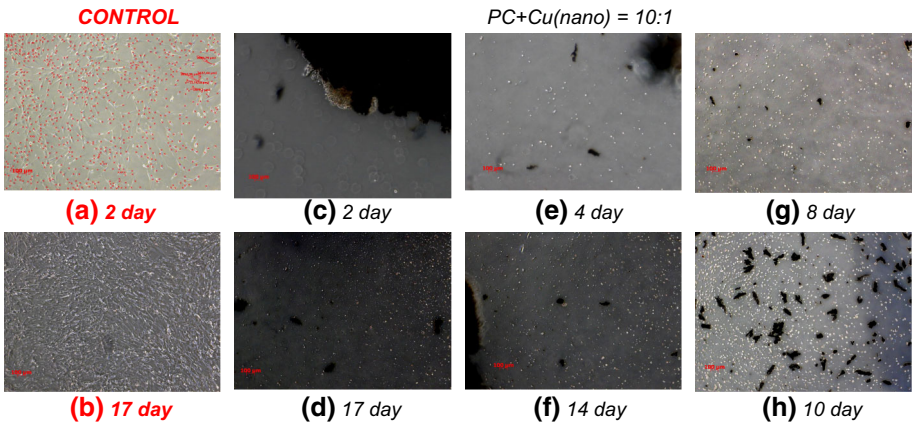

Fig. 6 17 day tests for PC-Cu/CuO system: **a**, **b** MMSC in nutrient mediums for control; **c–h** images of morphological analysis during 1–17 days

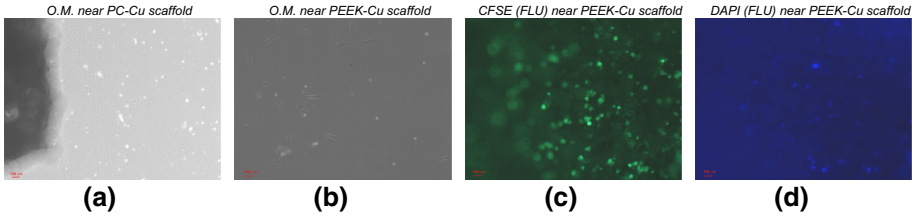

Fig. 7 Ten days tests for PC-Cu (**a**) and PEEK-Cu/CuO (**b**–**d**) systems: **a**, **b** O.M.—optical microscopy; **c** CFSE; **d** DAPI

4 Conclusion

The laser-assisted technique of the 3D synthesis was used to prepare porous PC or PEEK structures containing encapsulated copper nanoparticles, which were heterogeneity distributed over the sintered polymer. The obtained SEM and XRD data confirmed the formation of the Cu core—polymer shell structures around those nanoparticles.

The PC-Cu/CuO system demonstrated a direct toxic effect due to making the matrix alkaline and consequent death of the cells. The PEEK biocompatible matrix protects the MSSC from the apoptosis effects from the Cu-particles. Alternation of PEEK and PC matrices can be a way of regulating the cells' death, which is useful for medical applications (targeting and drug delivery systems).

Acknowledgement The study was supported by the grant of the Russian Science Foundation (Project No. 15-19-00208).

References

Chang, Y.N., Zhang, M., Xia, L., Zhang, J., Xing, L.: The toxic effects and mechanisms of CuO and ZnO nanoparticles. Materials **5**, 2850–2871 (2012)

Das, U.S., Wohlert, M., Beaman, J.J., Bourell, D.L.: Processing of titanium net shapes by SLS/HIP. Mater. Des. **20**, 115–121 (1999)

Engel, B., Bourell, D.L.: Titanium alloy powder preparation for SLS. Rapid Prototyp. J. **6**, 97–106 (2000)

Kanczler, J.M., Mirmalek-Sani, S., Hanley, N.A., et al.: Biocompatibility and osteogenic potential of human fetal femur-derived cells on surface selective laser sintered scaffolds. Acta Biomater. **5**, 2063–2071 (2009)

Leong, K.F., Phua, K.K.S., Chua, C.K., et al.: Fabrication of porous polymeric matrix drug delivery devices using the selective laser sintering technique. Proc. Inst. Mech. Engrs. Part H. **215**, 191–201 (2001)

Murray, P.E., García Godoy, C., García Godoy F.: How is the biocompatibility of dental biomaterials evaluated? Med. Oral Patol. Oral Cir. Bucal **12**(3), E258–E266 (2007)

Nirmalanandhan, V.S., Sittampalam, G.S.: Stem cells in drug discovery, tissue engineering, and regenerative medicine: emerging opportunities and challenges. J. Biomol. Screen. **14**(7), 755–768 (2009)

Ogura, N., Kawada, M., Chang, W., et al.: Differentiation of the human mesenchymal stem cells derived from bone marrow and enhancement of cell attachment by fibronectin. J. Oral Sci. **46**(4), 207–213 (2004)

Ott, M., Gogvadze, V., Orrenius, S., Zhivotovsky, B.: Mitochondria, oxidative stress and cell death. Apoptosis **12**, 913–922 (2007)

Salamon, A., Toldy, E.: Use of mesenchymal stem cells from adult bone marrow for injured tissue repair. Orv. Hetil. **150**(27), 1259–1265 (2009)

Shafagh, M., Rahmani, F., Delirezh, N.: CuO nanoparticles induce cytotoxicity and apoptosis in human K562 cancer cell line via mitochondrial pathway, through reactive oxygen species and *P53*. Iran. J. Basic Med. Sci. **18**(10), 993–1000 (2015)

Shishkovsky, I.: Laser synthesis of functional mesostructures and 3D parts. Fizmatlit Publ, Moscow (2009)

Shishkovskii, I.V., Yadroitsev, I.A., Smurov, IYu.: Selective laser sintering/melting of nitinol–hydroxyapatite composite for medical applications. Powder Metall. Met. Ceram. **50**(5/6), 275–283 (2011). doi:10.1007/s11106-011-9329-6

Shishkovskii, I.V., Morozov, YuG, Fokeev, S.V., et al.: Laser synthesis and comparative testing of a three-dimensional porous matrix of titanium and titanium nickelide as a repository for stem cells. Powder Metall. Met. Ceram. **50**(9/10), 606–618 (2012). doi:10.1007/s11106-012-9366-9

Shishkovsky, I.V.: SLS design of porous drug delivery system from porous nitinol. Nano- i mikrosistemnaya tekhnika **9**, 39–43 (2012)

Shishkovsky, I., Scherbakov, V.: Selective laser sintering of biopolymers with micro and nano ceramic additives for medicine. Phys. Proc. **39**, 491–499 (2012). doi:10.1016/j.phpro.2012.10.065

Volchkov, S.E., Tumina, O.V., Topovski, A.N., et al.: Comparative characteristics of MMSC from different sources. Cell Transplantol. Tissue Eng. **3**, 8–9 (2009)

Williams, J.M., Adewunmi, A.I., Schek, R.M., et al.: Bone tissue engineering using polycaprolactone scaffolds fabricated via selective laser sintering. Biomaterials **26**, 4817–4827 (2005)

Yang, H., Liu, C., Yang, D.F., Zhang, H.S., Xi, Z.: Comparative study of cytotoxicity, oxidative stress and genotoxicity induced by four typical nanomaterials: the role of particle size, shape and composition. J. Appl. Toxicol. **29**, 69–78 (2009)

Zinger, O., Anselme, K., Denzer, A., et al.: Time-dependent morphology and adhesion of osteoblastic cells on titanium model surfaces featuring scale-resolved topography. Biomaterials **25**(14), 2695–2711 (2004)